



Total Column Ozone Retrieval from Novel Array Spectroradiometer

Luca Egli¹, Julian Gröbner¹, Herbert Schill¹ and Eliane Maillard Barras²

¹Physikalisch-Meteorologisches Observatorium Davos, World Radiation Center (PMOD/WRC), 7260 Davos Dorf, Switzerland

²Federal Office of Meteorology and Climatology, MeteoSwiss, 1530 Payerne, Switzerland

Correspondence to: L. Egli (luca.egli@pmodwrc.ch)

Abstract

This study presents total column ozone (TCO) retrieval from a new system, called Koherent, developed at PMOD/WRC. The instrument is based on a small, cost effective, robust, low-maintenance and state-of-the-art technology array spectroradiometer. It consists of a BTS-2048-UV-S-F array spectroradiometer from Gigahertz-Optik GmbH, coupled with an optical fiber to a lens-based telescope mounted on a sun tracker for measuring direct UV irradiance in the ultraviolet wavelength band between 305 nm to 345 nm.

Two different algorithms are developed for retrieving TCO from these spectral measurements: 1) TCO retrieved by a minimal least squares fit algorithm (LSF) and 2) a Custom Double Ratio (CDR) technique using four specifically selected wavelengths from the spectral measurements. The double ratio technique is analogous to the retrieval algorithm applied for the Dobson and the Brewer but adopted and optimized here for TCO retrieval with Koherent. The instrument was calibrated in two different ways: a) absolute calibration of the spectra using the portable reference for ultraviolet radiation QASUME for the LSF retrieval and b) relative calibration of the extraterrestrial constant (ETC) of the CDR retrieval, by minimizing the slope between air mass and the relative differences of TCO from QASUME and Koherent. This adjustment of the ETC allows the instrument to be calibrated with standard TCO reference instruments during calibration campaigns, such as a double monochromator Brewer.

A two-year comparison in Davos, Switzerland, between Koherent and the Brewer 156 (double monochromator) shows that TCO derived from Koherent and the Brewer 156 agree in average over the entire period within less than 0.7% for all retrievals in terms of offset. The performance in terms of slant path depends on the selected retrieval and the applied corrections. The stray light corrected LSF retrieval exhibits a smaller slant path dependency than the CDR retrieval and performs almost as for a double monochromator system. The slant path dependency of the CDR is comparable to the slant path dependency of a single Brewer monochromator. The combination of both retrievals leads to performance with an offset close to zero compared to Brewer 156, a seasonal amplitude of the relative difference of 0.08% and a slant path dependency of maximum 1.64%, which is similar as other standard TCO instruments such as single Brewer or Dobson.

Applying the double ratio technique by selecting the wavelengths and slit functions from Brewer and Dobson, respectively, allow to determine the effective ozone temperature within 3 K on daily averages. With the improved TCO retrieval, Koherent serves as a new low maintenance instrument to operationally monitor TCO at remote sites. The presented TCO retrieval may be applied to other array based spectroradiometers providing direct spectral measurements in the ultraviolet.

1 Introduction

The depletion of the stratospheric ozone layer is observed since the 1970's (e.g. Molina and Rowland 1974, Solomon 1999, Staehlin et al. 2018) and reported in the World Meteorological Organisation (WMO) assessment of ozone depletion (e.g. WMO, 2018) on a quadrennial schedule. In order to monitor the evolution of the ozone layer, accurate instrumentations such as the Dobson spectroradiometer (Dobson, 1968, Komhyr et al., 1989) and the Brewer spectroradiometer (Kerr et al. 1981)



have been developed to ensure worldwide long-term observations of total column ozone (TCO) forming a global network. The ozone layer absorbs solar ultraviolet radiation at wavelengths shorter than 350 nm and protects life on Earth's surface from harmful UV radiation. A spectroradiometer allows retrieving TCO by accurately measuring direct sun irradiance at the Earth's surface in the UV wavelength band and by using an atmospheric model based on the Beer-Lambert Law (Kerr et al., 1988). In the Dobson instruments, prisms are selecting the four specific wavelengths which are used for the ozone retrieval (Evans, 2008). Most of the Dobsons are manually operated and require therefore substantial manpower for the operation at remote sites. The three Swiss Dobsons used in this study have been automated (Stübi et al. 2021). In the 1980's the Brewer spectroradiometer (Kerr et al., 1981, Kerr et al. 1985) was developed as an automatic device measuring direct solar UV radiation with gratings instead of prisms. The first instruments were single monochromator with one grating to select the wavelengths at the specific slits. Later in the development, Brewers were equipped with two gratings to form double monochromator instruments. Double monochromator devices perform UV measurements with insignificant stray light impact, contrary to single monochromator Brewers or to Dobson, which suffer from stray light at high solar zenith angles and corresponding high air masses. The Brewers were formed to a network of automatic stations, which required few operational manpower as an advantage for remote sites, but still require regular maintenance by trained experts. For the Dobson and the Brewer spectrophotometers, the retrieval of TCO is obtained by the double ratio technique at four specific wavelengths in the UV absorption band (see section 2.2 and Gröbner et al., 2021). Redondas et al. (2014) and Gröbner et al. (2021), showed that the best consistency between TCO from Brewer and Dobson can be achieved by using the G14 ozone absorption cross section (Serdyuchenko et al., 2014) and the inclusion of effective ozone temperature from balloon soundings for the Dobson retrieval. Both instruments require the extraterrestrial constant (ETC), which defines the irradiance ratio at the top of the atmosphere, as a parameter of the retrieval. This parameter is determined by Langley plot calibration at some specific sites with stable atmospheric conditions (Mauna Loa, Hawaii, US and Izaña, Tenerife, Spain) or it is determined by on-site comparison with a regional reference instrument (Köhler et al. 2002, Redondas et al. 2019). In the framework of the Global Atmosphere Watch program (GAW), WMO defined the Brewer and the Dobson instruments as the standard instruments for TCO monitoring from Earth's surface. In recent years, other instruments measuring direct solar irradiance between 300 nm and 340 nm were developed to retrieve TCO, without the requirement of on-site calibration by reference instruments. In particular array spectroradiometers have the advantage that a continuous spectral range is measured instead of only discrete wavelength values as by the Brewer or the Dobson. The instruments are small, robust, require low maintenance during their operation and acquire spectra within a time frame of seconds. However, it is also reported that array spectroradiometers suffer from stray light due to the single monochromator setup (Egli et al., 2016). An example of an array spectroradiometer based system is the Pandora system, which form a global network for atmospheric composition measurements, including TCO (Herman et al. 2017). The instrument measures solar spectra with an array spectroradiometer and an input optic connected by a fiber to the spectroradiometer. TCO is retrieved by a spectral fitting algorithm wavelength band between 305 nm and 330 nm. Comparison with Dobson instrument shows an averaged difference of $2.1 \pm 3.2\%$ (Herman et al. 2017) with the Pandora system. Herman et al. (2017) reported that TCO have been corrected for the impact of effective ozone temperature and for the influence of straylight. Similarly as Pandora, the entrance optics of the Phaeton system consists of a fiber coupled telescope connected to an array spectroradiometer (Kouremeti et al., 2008). The spectral measurements from Phaeton are used to retrieve TCO by a DOAS/MAXDOAS technique using the wavelength band between 315 nm and 337 nm. Averaged biases of $0.94\% \pm 1.26\%$ of TCO from Phaeton are observed by comparison with a Brewer single monochromator spectroradiometer when using the effective ozone temperature as input for the retrieval (Gertski et al., 2018).

The BiTecSensor (BTS) array spectroradiometer from Gigahertz Optik GmbH (Zuber et al., 2018a) reduces straylight by filtering solar radiation with different bandpass filters inside the array-spectroradiometer (Zuber et al. 2021). Contrary to the



aforementioned systems the “BTS Solar” is based on a BTS array spectroradiometer unit with directly mounted diffusor
85 entrance optic and a tube for field of view limitation for irradiance measurements instead of a fiber coupled telescope (Zuber
et al., 2018b and Zuber et al 2021). The retrieval algorithm is based on the comparison from two selected wavelength bands
(307 nm to 311 nm and 319 nm to 324 nm) of the measured data with a lookup table pre-calculated by the libRadtran
software package for radiative transfer calculations (Emde et al., 2016). The look-up table is pre-calculated for a specific
location and requires ground pressure for correction but does not use the effective ozone temperature. A long-term
90 intercomparison in 2019 and 2020 of the BTS Solar at Hohenpeissenberg, Germany, showed a bias of less than 0.1% with a
standard deviation of less than 0.8% compared to Brewer using the Bass and Paur cross section. Stray light effects of BTS
are discussed and reported to be minor for TCO retrieval by the look-up table technique (Zuber et al., 2018a, Zuber et al.,
2018b and Zuber et al 2021). Also in Zuber et al., (2021), the Koherent system operated at PMOD/WRC was introduced as
an instrument which connects the BTS array spectroradiometer by an optical fiber to a lens-based telescope (see section 2.1).
95 In analogy to Huber et al., (1995) and Egli et al., (2022) a least square (LSF) spectral fitting algorithm (see section 2.2) is
applied for TCO retrieval during 2019 and 2020 in Davos, Switzerland. TCO from the LSF technique exhibit an averaged
bias of 1.7% with a standard deviation of 1.4% and a seasonal cycle of about 2% (Zuber et. al. 2021). The LSF algorithm
displayed a first version of LSF applied for array spectroradiometer and did not include the effective ozone temperature as
input in the retrieval. Zuber et. al. (2021) discussed if the seasonal cycle is attributed to remaining straylight effects or to the
100 retrieval at constant effective ozone temperature of 228 K through the seasons. However, it remained unclear which effect
caused the seasonal cycle.

Recently, Egli et al., (2022) presented traceable TCO measurements from the world portable reference spectroradiometer for
UV radiation QASUME (Gröbner et al. 2005). QASUME consists of a scanning double monochromator measuring direct
solar UV spectral irradiance at wavelength between 305 nm and 345 nm. QASUME is fully characterized in the laboratory
105 with sources that are traceable to primary SI standards with an unbroken calibration procedure and a comprehensive
uncertainty analysis for the entire calibration chain (Hülßen et al., 2016 and Gröbner et al., 2017). TCO from these high-
quality direct UV spectral measurements are used for an improved, standardized and optimized LSF retrieval algorithm in
the wavelength band between 305 nm and 345 nm. In Egli et al., (2022) the standard LSF retrieval is described in detail and
is also considered here as the standard retrieval for traceable TCO measurement from spectral solar measurements. A long-
110 term comparison of QASUME TCO with a Brewer double monochromator and a Dobson in Davos, Switzerland showed an
offset of about 1% and a seasonal cycle of less than 0.2%. This small seasonal variation indicates the proper inclusion of the
effective ozone temperature for QASUME LSF retrieval and the negligible impact of straylight.

This study aims first to apply the standard LSF retrieval algorithm to spectral measurements from the BTS array-
spectroradiometer system Koherent including the effective ozone temperature to investigate potential stray light effects of
115 Koherent. Second, the measured spectra of Koherent are used to apply a custom double ratio (CDR) technique (in analogy to
the Dobson and Brewer retrieval) to further improve the performance of Koherent. The study also investigates the potential
of the double ratio technique applied at Koherent to retrieve the effective ozone temperature from ground-based
measurements as shown in Kerr et al. (2002).

The results of TCO from Koherent calculated by the standard LSF and the CDR technique are compared with the double
120 monochromator Brewer 156 of MeteoSwiss, operated at the World Radiation Center (PMOD/WRC), in Davos, Switzerland.
The comparison during the period from 1 October 2019 to 30 September 2021 allows validating the performance of
Koherent and selecting the best retrieval for operational use. The overall objective is to obtain continuous TCO observations
from a small, robust and low maintenance instrument for remote sites with unattended operation.



2 Instrument and Retrieval Algorithm

125 2.1 Koherent array spectroradiometer based instrument

The transportable system Koherent was built as a research instrument to test the ability of a novel, array spectroradiometer for continuous TCO monitoring. As described in Zuber et al. (2021), Koherent is based on a fiber coupled BTS-2048-UV-S-F array spectroradiometer, which is connected to a lens-based imaging telescope (Picture 1). The telescope with a field of view of about $\pm 0.6^\circ$ is mounted on a sun tracker following the sun to measure direct solar irradiance at the measurement platform at PMOD/WRC, Davos, Switzerland at 1560 m a.s.l. (coordinates: 46.81 N, 9.83 E). The small array spectroradiometer is enclosed in a temperature stabilized weather-proofed box to ensure a constant temperature through all seasons of the year. The BTS is controlled with a python software-routine on an embedded computer inside the box. The raw data is stored immediately on the embedded computer and transferred to an external server on a five minute schedule. During the operation between 2019 and 2021, the system performed reliably in more than 99% of all days and can be considered as technically mature. The time interval of each reading is usually 1 minute since the device needs around 45 seconds for one measurement. However, at conditions with low direct sun irradiance intensity (e.g. cirrus clouds or high solar zenith angles), around 150 seconds are needed due to increased integration time (Zuber et al. 2021). Since the airmass can change rapidly at high solar zenith angles, higher integration times than 150 sec were not permitted in the measurement program. For example, using 45 seconds integration time, the airmass changes by 0.35% at airmass 3.5 (or SZA of around 75°) and to 1.15 % for integration times of 150 seconds leading to an uncertainty of TCO of the same relative amount.

The postprocessing to prepare the spectra for TCO retrieval was performed off-line with the following steps:

First, converting the raw-counts of the readings to irradiance using in-situ calibration, with the world reference for UV radiation QASUME (Gröbner et al., 2005, Hülsen et al., 2016 Gröbner et al., 2017). Spectral measurements of QASUME are traceable to the primary spectral irradiance standard of the Physikalisch Technische Bundesanstalt (PTB) (Gröbner and Sperfeld, 2005) via secondary standard tungsten halogen 1 kW FEL lamps. The stability of QASUME is monitored in the field with 250 W tungsten halogen lamps on the measurement platform (Egli et al., 2022). The responsivity from Koherent was calibrated by the spectra from QASUME at local noon using data from four clear sky days between 5 and 15 of September 2020, when the sun irradiance was as stable as possible over time. This in-situ calibration was used for all other days of the two years period. Zuber et al., (2021) highlighted the difficulties of laboratory calibration of the telescope entrance optics with poor reproducibility of the calibration. Therefore, the direct in-situ calibration with the world UV reference QASUME was chosen for most of the results of this study. The lamp calibration will later be used when adjusting the ETC in the double ratio technique (section 3.2 b). Figure 1 displays the ratio between synchronous spectra from QASUME and Koherent for individual wavelength bands normalized to local noon (12 UTC), exhibiting an increase for all wavelength longer than 310 nm of +2% between SZA 60° and 70° . The wavelength band at 305 nm increases up to 4% at high solar zenith angles. The larger increase at 305 nm is a sign of stray light impact at shorter wavelengths, which will be addressed and discussed later.

The second step of the post processing chain, consisting in a wavelength shift correction and spectrum homogenization using the MatSHIC software developed at PMOD/WRC (Egli et al., 2022), was applied to the Koherent spectrum to obtain a standard spectrum for further retrieval of TCO. For this study, the resulting spectra were homogenized to 0.01 nm wavelength-increment and convolved with a triangular slit function of 0.5 nm full width half maximum for the least square (LSF) fit algorithm (see section 2.2) and to 0.1 nm for the custom double ratio technique (section 2.3), respectively. The so homogenized spectra were used to retrieve TCO with the following algorithms.



2.2 Least Square (LSF) fitting algorithm

Egli et al. (2022) presented a standardised algorithm to retrieve TCO from spectral irradiance measurements. The same algorithm, thoroughly tested in Egli et al. (2022), is applied here for TCO retrieval from Koherent. The algorithm used here differs from the algorithm used in Zuber et al. (2021) by the inclusion of the effective ozone temperature as input parameter and differs in other specific settings (e.g. solar spectrum TSIS, Coddington et al., 2021).

In summary, the LSF algorithm is using a spectral non-linear least square fitting procedure in the wavelength range between 305 nm to 345 nm and implements an atmospheric model based on the Beer-Lambert law:

175

$$I_{\lambda}(T, p, O_3) = I_{\lambda}^0 \exp[-(\tau_{\lambda}^{O_3}(T) \cdot m^{O_3} + \tau_{\lambda}^{AOD} \cdot m^{AOD} + \tau_{\lambda}^R(p) \cdot m^R + \tau_{\lambda}^{SO_2} \cdot m^{SO_2})] \quad \text{Eq.1}$$

I_{λ} denotes the modelled spectral irradiance at the wavelength λ . I_{λ}^0 indicates the TSIS solar reference spectrum at the top of the atmosphere (Coddington et al., 2021), while the airmass m , denotes the path length of radiation through the atmosphere.

180 The atmospheric model accounts for the effect of ozone absorption at each wavelength and furthermore the attenuation by the atmosphere including aerosols, Rayleigh scattering and Sulfur Dioxide (SO₂). The resulting attenuated modelled solar spectrum using Eq. 1 is then compared with the measured solar spectrum by Koherent, by minimizing the spectral residuals between the modelled and measured solar spectrum and returns the corresponding model parameters including TCO (Egli et al., 2022).

185 For the term of ozone attenuation $\tau_{\lambda}^{O_3}(T) \cdot m^{O_3}$ in Eq. 1, the SG14 ozone absorption cross section (Serduychenko et al. 2014, Egli et al. 2022) for different effective ozone temperatures (T) is used in the retrieval algorithm. TCO retrieved with SG14 shows a dependency on effective ozone temperature of 0.1%/K (Egli et al. 2022). This implies, that the effective ozone temperature is required as input for the TCO retrieval algorithm to achieve uncertainties in retrieved TCO of less than about 1%. In analogy to Gröbner et al. (2021) and Egli et al. (2022), the effective ozone temperature retrieved from balloon
 190 sounding at the nearest sounding station in Payerne, Switzerland, is taken as daily input for the retrieval algorithm. The term $\tau_{\lambda}^{AOD} \cdot m^{AOD}$ in Eq. 1 denotes the attenuation by aerosol optical depth. The wavelength dependence of the aerosol optical depth is parametrized linearly, normalized to 340 nm. The term $\tau_{\lambda}^R(p) \cdot m^R$ of Eq. 1 accounts for the effect of Rayleigh scattering in the atmosphere, which is parametrized according to Bodhaine et al. (1999) and requires the air surface pressure p which is selected from the pressure climatology in Davos as 820 hPa. Finally, the attenuation by SO₂ is also considered in
 195 the overall attenuation equation (Eq.1), even though the amount of SO₂ in the atmosphere above Davos is insignificant (Gröbner et al., 2021). Accounting for all four terms of attenuation in the Beer-Lambert atmospheric model, the LSF approach derives the best fit to the unknown parameters AOD and TCO.

2.3 Custom Double Ratio (CDR) Technique

200

A second approach to retrieve TCO from the spectral measurements is to apply the double ratio technique from four specific wavelength as used for the Brewer TCO retrieval (Kerr et al., 1985). Spectral measurements from Koherent allow to select specific wavelengths from the measured spectrum and to apply the double ratio technique as for the Brewer.

According to Gröbner et al. (2021), who summarized the double ratio technique for Brewer and Dobson, we present here the principle of the custom double ratio (CDR) technique for Koherent as follows:

205

In analogy to the LSF retrieval, the absorption through the atmosphere is based on the Beer-Lambert Law (Eq. 1). The equation can be rewritten for the CDR technique as:

$$\tau_{\lambda} = \frac{\log I_0^{CDR}(\lambda) - \log I^{CDR}(\lambda)}{m} \quad \text{Eq. 2}$$



Were I is the measured spectrum, I_0 is the top of atmosphere reference spectrum and τ_λ is the total optical depth from the
 210 different absorption and attenuation terms. Contrary to Eq. 1 where λ indicates each individual wavelength of the measured
 spectrum, λ denotes one of the four wavelengths for the double ratio technique. For the CDR we have selected the four
 wavelengths: $\lambda_i^{CDR} = [310, 322, 332, 345] \text{ nm}$ to obtain a significant sensitivity to ozone absorption. Moreover, $I^{CDR}(\lambda)$ is
 not the solar irradiance at only one specific wavelength of the measured spectrum, it indicates the integral of the spectrum
 over defined slit functions $s_i(\lambda)$ (Figure 2 and Eq. 3) with the center-wavelength at λ_i^{CDR} .

215

$$I_i^{CDR}(\lambda) = \frac{\int I_i(\lambda) \cdot s_i(\lambda) d\lambda}{\int s_i(\lambda) d\lambda} \quad \text{Eq. 3}$$

The index *CDR* indicates the integral over the slit function $s_i(\lambda)$ (Eq. 3), not only of the measured spectrum, but later also of
 the solar spectrum, the ozone absorption cross section and the Rayleigh scattering. The slit functions $s_i(\lambda)$ for the CDR are
 220 rectangular slit functions with the width of 1 nm for the wavelength 310 nm and 322 nm ($i=1,2$) and the width of 4 nm for
 the wavelengths 330 and 345 nm ($i=3,4$), respectively (see Figure 2, blue rectangles). The different sizes of the widths for
 shorter and longer wavelengths are chosen in analogy to the Dobson slits, where the width at shorter wavelengths is about 1
 nm and about 4 nm at longer wavelengths.

As stated in Gröbner et al. (2021), the effect of Sulphur dioxide and nitrogen dioxide can be neglected for the atmosphere in
 225 Davos. However, the attenuation from Rayleigh scattering $\tau_\lambda^R(p) \cdot m_\lambda^R$ needs to be subtracted from the total optical depth τ
 to retrieve the optical depth for ozone in the UV band:

$$\tau_{O_3}(\lambda, T, p) = \alpha(\lambda, T) \cdot TCO \cdot m^{O_3} = \frac{\log I_0^{CDR}(\lambda) - \log I^{CDR}(\lambda) - \tau_\lambda^R(p) \cdot m_\lambda^R}{m^{O_3}} \quad \text{Eq. 4}$$

230 Where m^{O_3} and m^R are the effective airmass of ozone and Rayleigh-scattering and $\alpha(\lambda, T)$ is the SG14 cross section
 depending on effective ozone temperature as described later. The influence of absorption and scattering by aerosols in the
 atmosphere is minimized by using ratios of measurements at close wavelengths (Gröbner et al. 2021). TCO is then retrieved
 by a linear combination of the measurements, the solar spectrum and the Rayleigh scattering term from the four specific
 wavelengths λ_i^{CDR} ,

235

$$TCO = \frac{F^{CDR} - F_0^{CDR} - \Delta\beta \cdot m^R}{\Delta\alpha \cdot m^{O_3}} \quad \text{Eq. 5}$$

where $F^{CDR} = \sum_{i=1}^4 w_i \cdot \log I^{CDR}(\lambda_i^{CDR})$ is the logarithmic sum of the solar irradiance. Accordingly, the terms for the top of
 the atmosphere solar irradiance F_0^{CDR} is calculated by the weighted sum of logarithmic solar reference spectrum TSIS
 (Coddington et al., 2021). For the CDR algorithm used here, the weights are equally chosen in analogy to the Dobson
 240 retrieval $w_i^{CDR} = [+1 -1 -1 +1]$ to calculate the ratios of measurements for best performance. Finally, for consistency with
 units TCO in Eq. 5 was multiplied by the factor 1000.

The ozone absorption coefficient α_i at wavelength λ_i is derived by the SG14 (Serdruchenko et al., 2014) cross section
 $SG14(\lambda, T)$, where T is the effective ozone temperature from balloon soundings in Payerne, Switzerland (see section 2.2).
 The ozone absorption coefficient is calculated for the four wavelengths by the same convolution as described in Eq. 3,
 245 replacing $I_i(\lambda)$ by $SG14(\lambda, T)$.

The weighted ozone absorption coefficient $\Delta\alpha$ for Eq. 5 is then derived by the weighted sum of α_i : $\Delta\alpha = \sum_{i=1}^4 w_i \cdot \alpha_i$.



The Rayleigh attenuation term $\Delta\beta$ for Eq. 5 is calculated again based on Eq. 3 and the weighted sum by replacing $I_i(\lambda)$ by the parametrization according to Bodhaine et al. (1999), requiring the climatological air surface pressure $p = 820$ hPa in Davos, Switzerland, as input.

250 The algorithm presented above can also be adapted to apply a double ratio Brewer retrieval with Koherent spectra, when using the trapezoidal slit functions of the Brewer with full width half maximum (FWHM) of around 0.55 nm at wavelengths $\lambda_i^{Brewer} = [310.0, 313.5, 316.8, 320.1]$ nm (Figure 2, green lines) with weightings of $w_i^{Brewer} = [+1 -0.5 -2.2 +1.7]$ (Gröbner et al. 2021).

255 Analogous, the Dobson retrieval can be applied by using the measured slit functions of the automated Dobson D101 (Stübi et al. 2021) derived from a tuneable and portable radiation source (TuPS, Smid et al., (2020)). The measurement of the slit functions revealed center-wavelengths of $\lambda_i^{Dobson 101} = [305.4, 324.9, 317.4, 339.7]$ and FWHM of around 1 nm for the two shorter wavelengths and around 4 nm for the two longer wavelengths (Köhler et al., 2018). The slit functions are shown in Figure 2 for the Brewers (trapezoidal slit functions), the Dobsons (measured by TuPS) and the rectangular shapes for the CDR technique introduced here. The slit functions, center-wavelengths and the weightings of the CDR retrieval differ from
260 the Brewer or Dobson wavelengths and are customized for Koherent for best performance of the CDR retrieval with Koherent. The performance will be presented and discussed in the following section.

3 Results and Discussion

265 The results of TCO from Koherent are compared with TCO from the Brewer 156 double monochromator operated at PMOD/WRC. Due to the long-term quality assurance and strong straylight suppression of the Brewer 156, the instrument was chosen to serve as a reference for the two-year period between 1 October 2019 and 30 September 2021. Additionally, some aspects of Koherent are compared with two single Brewers 040 and 072 and Dobson 101 from MeteoSwiss operated at PMOD/WRC. Koherent, Brewer 072 and the Dobson 101 were co-located in Davos, Switzerland, during the entire period of
270 comparison. Brewer 040 moved to Davos in February 2021. Following Gröbner et al. (2021), TCO from the Brewer instrument is calculated with the SG14 cross-section. The following graphs show the relative differences of quasi simultaneous TCO within a five-minute interval in relation to TCO from the Brewer 156 indicated in percent. The missing “period” of TCO comparisons in the figures are attributed due to some testing of Koherent and have been removed from the comparison.

275 In the following, the comparison is quantified in terms of offset, which indicates the averaged differences between the instruments, seasonal amplitude, which shows the amount of seasonal effect by displaying a sinusoidal fit to the differences. The slant path dependency is the relation between the relative differences and the ozone slant path column, which is defined as the product of TCO and airmass. To quantify the ozone slant path dependency, the difference of maximum and the minimum of the quadratic fit in the slant path column between 300 DU and 1200 DU is calculated.

280

3.1 LSF retrieval

a) Wavelength range 305 nm to 345 nm

285 Table 1 lists the comparison of TCO between Brewer 156 and Koherent when applying the LSF retrieval and using the spectral range between 305 nm and 345 nm for the spectral fitting. The results show that in average over the entire period, Koherent slightly overestimates TCO with an offset of 0.26%. However, a significant seasonal amplitude of 1.17% is observed as well. Zuber et al. (2021) compared Koherent to the double monochromator Brewer 163 using a first version of the LSF algorithm without taking into account the effective ozone temperature as input parameter and using the Bass and Paur cross-section (Bass and Paur, 1985). Their results show a standard deviation around 2.72 % with an offset of -1.64%



290 and a seasonal amplitude of around 2%. Our result indicates that the inclusion of the effective ozone temperature improves the agreement of Koherent and Brewer double monochromator.

Figure 3 displays the dependency of the relative differences on the ozone slant path column. The circles are averages of the five minute values between intervals of 100 DU of ozone slant path column. The lines are a quadratic fit of the five minute values, which are not shown in the Figure. The graph shows a strong dependency of the relative TCO differences with ozone
295 slant column of 4.42% (Table 1). This figure and the seasonal cycle indicate that the biases are larger at higher air masses or high solar zenith angles. The observed seasonal cycle may be caused by straylight at shorter wavelengths. This hypothesis is supported by the results in Figure 1 (lower panel), where solar spectra from Koherent deviate more at shorter wavelengths (305 nm) than at wavelengths longer than 310 nm with respect to the QASUME solar reference spectra. In order to further support this hypothesis, the wavelength range of the LSF retrieval was changed to 310 nm to 345 nm.

300

b) Wavelength range 310 nm to 345 nm

Restricting the wavelength range from 310 nm to 345 nm, the seasonal cycle can be reduced to 0.86% with an offset close to zero (Table 1). Figure 3 also shows a lower ozone slant path dependency of 2.18% between maximum and minimum than for the 305 nm to 345 nm wavelength range. As shown in Figure 1 at low solar zenith angles (SZA), all wavelength regions are
305 within 0.5%. At higher SZA ($> 60^\circ$), the wavelength region around 305 nm deviates up to 2% (at SZA 70°) compared to the other wavelengths. This spectral bias explains the slant path dependency change when restricting the wavelength range to 310 nm to 345 nm.

As shown in section 2.1, the measuring-time for each spectrum can vary from 45 seconds up to 150 seconds. The longer measurement-time of 150 seconds at airmass of 3.5 leads to airmass changes up to 1.15 % during this time span. This effect
310 may also contribute to the observed slant path dependency but is minor compared to the contribution of stray light.

c) Stray light correction

An alternative method to account for the effect of stray light is to apply a correction on the TCO retrieved by LSF. For this purpose, four full clear sky days between 5 and 15 September 2022 were chosen to parametrize the slant path dependency
315 between the LSF retrieved TCO of QASUME (Egli et al. 2022) and the LSF retrieved TCO of Koherent by a linear fit. Both LSF retrievals used the wavelength range between 305 nm and 345 nm. The coefficients of this linear fit were then applied to all LSF retrievals from Koherent for the entire two years period. Figure 3 (red line) shows a resulting improved slant path dependency of 0.46%. For comparison, the slant path dependency between the two double monochromator instruments Brewer 156 and QASUME is displayed in Figure 3 (grey line). The maximal difference between the 2 instruments shown by
320 the grey line in Figure 3 is 0.18% (Table 1) which is similar to the slant path dependency between two Brewer double monochromator of 0.35% (Brewer 163 vs. Brewer 156, Table 1) and is in the range of the stray light corrected LSF retrieval. However, the red circles in Figure 3 show that the slant path dependency of stray light corrected Koherent LSF is similar to the QASUME-Brewer 156 comparison restricted to ozone slant path between 300 and 900 DU. For ozone slant path higher than 900 DU, Koherent shows a significant bias, which is not observed between the two double monochromator Brewers.

325

3.2 Custom double ratio technique

a) CDR from calibrated spectra

As described in section 2.3, TCO can also be retrieved by the CDR technique using the four specific wavelengths and the rectangular slit functions (Figure 2). Table 1 presents the results of the two-year comparison of Koherent CDR with the
330 Brewer 156 double monochromator. The amplitude of the seasonal cycle is about 0.17% with an offset of 0.02%. This low amplitude is substantially reduced compared to the LSF retrieval. Figure 4 blue circles and line shows the relative



differences between TCO of Brewer 156 and Koherent dependent on the ozone slant path. The minimum to maximum dependency of the quadratic fit on the slant path is around 2.1% (Table 1).

335 For comparison, Figure 4 gray circles and line shows the slant path dependency of the relative differences between Brewer 156 and the single monochromator Brewer 072. The maximum to minimum of the quadratic fit of the data reveals a slant path dependency of 2.53% (Table 1). Table 1 also lists the slant path dependency of single monochromator Brewer 040 with Brewer 156 which is 1.52%. The performance of Koherent CDR lies between the two single Brewers 040 and 072, which indicates that the TCO retrieval from Koherent CDR performs at least as good as from a single Brewer monochromator, with

340 respect to ozone slant path. This CDR retrieval algorithm does not require any field calibration of TCO by adjusting the extraterrestrial constant (ETC) or the ozone absorption coefficient with a reference instrument as it is required for the standard double ratio technique with Brewer or Dobson. Instead, this CDR algorithm requires only a one-time vicarious calibration of the spectra with QASUME, the laboratory measured ozone cross sections (IUP, Serdyuschenko et al. 2014), Rayleigh scattering absorption coefficients (Bodhaine et al., 1999) and the space borne top-of-atmosphere solar reference

345 spectra (Coddington et al. 2021) for the extraterrestrial constant (F_0^{CDR} , Eq. 5).

b) CDR with adjusted ETC

Since CDR is analogous to the Brewer and Dobson retrieval algorithm, which requires the determination of the extraterrestrial constant by comparison with a reference instrument (Redondas et al. 2019, Komhyr 1989), F_0^{CDR} (Eq.5)

350 could also be determined by an intercomparison with a reference instrument. For Dobsons, only the ETC is adjusted according to the reference Dobson, since the ozone absorption coefficient is set to a nominal value (Komhyr, 1989). For Brewers, the adjustment of ETC is provided by a dedicated reference Brewer e.g. from the Regional Brewer Calibration Center Europe (RBCC-E) by periodic in-situ intercomparison campaigns (Redondas et al., 2019). Since the reference Brewer is calibrated on an absolute scale and the ozone absorption coefficient may vary specifically for each instrument, not only the

355 ETC, but also the absorption coefficient $\Delta\alpha$ (Eq. 7) can be adjusted in a so called two-point-calibration, where both the ETC and the ozone absorption coefficient are retrieved from the intercomparison with a reference Brewer. The same calibration procedure could therefore be applied to the Koherent CDR algorithm, which is also determined by the two parameters: extraterrestrial constant F_0^{CDR} and the absorption coefficient $\Delta\alpha$.

In order to avoid the calibration and validation with the same instrument, we have chosen an alternative approach to

360 determine the ETC for Koherent by using QASUME as a reference and validating the resulting TCO with Brewer 156. Since changes of the ETC affect the ozone slant path dependency, the adjustment of Koherent's ETC is performed by minimizing the slope of the dependency between air mass and the relative difference of QASUME and Koherent. Using the laboratory-based calibration of Koherent instead of the QASUME in-situ calibration, four clear sky days between 5 and 15 September 2020 have been chosen to adjust the extraterrestrial constant F_0^{CDR} of Koherent in comparison with QASUME. This

365 adjustment displays a relative calibration using the relative differences of QASUME and Koherent only. To avoid the inclusion of absolute TCO of this calibration we have further chosen the air mass only as a regression parameter instead of the slant path. Finally, to further minimize the effect of stray light from Koherent, an air mass range less than 2 for minimizing the slope is used.

The so adjusted ETC was used in the CDR algorithm to test the performance of the procedure. The two-years comparison to

370 Brewer 156 of Koherent TCO retrieved by CDR with the adjusted ETC shows an offset of -0.59% and a seasonal amplitude of 0.34% (Table 1) and is therefore well within the performance of the other retrievals (Table 1) or within comparisons of Arosa/Davos Brewers (Stübi et al. 2017 a,b). Figure 4 green circles and green line show that the slant path dependency of around 2% from maximum to minimum, which is similar as for the CDR retrieval and which is also less than the performance of Brewer 072 (Figure 4, grey circles and line). The adjustment of the ETC by minimizing the slope of the air

375 mass dependency is not a standard method but is used here as an alternative method for determining the ETC with QASUME



without any QASUME spectral or absolute TCO calibration. However, as aforementioned, the CDR algorithm can be calibrated with well-established calibration procedure if a network reference instrument such as the Brewer from RBCC-E is available (Redondas et al., 2019). This study shows that some calibration days during a field campaign are sufficient to obtain an ETC calibration which is stable over the two years.

380

3.3 Combining LSF and CDR

Since the methods presented in section 2 are different, but scientifically valid approaches, and since the validation with Brewer 156 showed comparable results, the three methods (LSF, CDR and ETC adjusted CDR) were merged to obtain a combined dataset of TCO from Koherent, by averaging all TCO values from the three methods. We have merged the stray light corrected LSF, the CDR and the ETC adjusted CDR dataset to one combined dataset. Figure 5 shows the entire temporal course between 1 Oct 2019 and 30 September 2021 of combined TCO. The small blue points indicate the five minutes measurements and the light blue circles monthly averages. The offset between combined TCO and Brewer 156 is close to zero with a seasonal amplitude of 0.08%. Figure 4 red circles and line and Table 1 additionally highlights that the slant path dependency is comparable to the performance of a single monochromator Brewer. The averaging of the three different retrievals results allows determining the standard deviation of each retrieval. The grey area in Figure 5 indicates the mean relative standard deviation of the individual retrieval to their average. The resulting 0.88% can be considered as the lower level of uncertainty ($k=1$) of TCO retrieved by Koherent when using different methods and calibration procedures.

As described in section 2, the effective ozone temperature is required for all TCO retrievals from Koherent measurements. The dependency on effective ozone temperature of the LSF retrieval is around 0.1%/K, which is in line with the temperature dependency of traceable TCO measurements with QASUME (Egli et al., 2022) or the effective temperature dependency of Dobsons TCO (Redondas et al., 2014). The CDR technique exhibits a slightly larger effective ozone temperature dependency of 0.16%/K. In order to account for this temperature dependency, $\Delta\alpha = 0.7513$ in Eq. 5, needs to be corrected by applying 0.16%/K of the effective ozone temperature measured by balloon soundings (Gröbner et al., 2021) or from ECMWF reanalysis data (<https://www.temis.nl/climate/efftemp/overpass.php>, last access: 23 November 2022). However, as will be described in the following section, the effective ozone temperature can be directly retrieved by Koherent.

3.4 Correlation with effective ozone temperature

Redondas et al. (2014) reported that the specific wavelength settings and the weighting for the double ratio technique of the Brewer retrieval led to a low sensitivity of TCO to effective ozone temperature. Kerr (2002) demonstrated that the effective ozone temperature can be retrieved from Brewer data with the group-scan method analysing different wavelength settings of the Brewer. Redondas et al. (2014) and Gröbner et al., (2021) also showed a sensitivity on effective ozone temperature of about 0.1%/K for the Dobson retrieval. In other words, if TCO is retrieved with a constant effective temperature for Brewer and Dobson, a seasonal cycle depending on the seasonal variation of the effective ozone temperature is observed (Redondas et al., 2014). As mentioned in section 2.3 the CDR technique can also be applied using the different Dobson and the Brewer settings in terms of specific wavelengths, slit functions and weightings (Gröbner et al., 2021).

Here, we estimate the differences in TCO by applying the double ratio technique using the Brewer and the Dobson different wavelength and slit function settings on Koherent spectra for a constant effective ozone temperature of 228 K, in order to investigate the potential of retrieving effective ozone temperature. The relative difference between TCO from the Brewer and the Dobson settings show a strong seasonal cycle of 3.9% amplitude (not shown). The amplitude of the differences between Brewer and Dobson settings used in the CDR retrieval correlates with the effective ozone temperature as shown in Figure 6. Since effective ozone temperature is commonly given on a daily schedule (e.g. ECMWF reanalysis data or



interpolated from balloon soundings (Payerne), the differences in effective ozone temperatures derived from the Brewer and
420 Dobson settings in the CDR retrieval are averaged to daily values to reduce the variability of the individual five minute
values. Figure 6 displays a linear fit to the data. The linear fit gives a sensitivity of the TCO on effective ozone temperature
of 0.52%/K. Based on the linear parametrization, the effective ozone temperature can be reconstructed from the differences
of the TCO retrieved from Koherent spectra applying the Brewer and Dobson settings for the double ratio technique. As
shown in Figure 7, the so determined effective ozone temperature agrees with the balloon sounding within a standard
425 deviation of circa 3 K. For comparison, the effective ozone temperature from ECMWF reanalysis data generally agrees with
balloon sounding within 2.5 K (Gröbner et al. 2021). Estimates of the effective ozone temperature with Koherent show a
larger day-to-day variation than balloon soundings measurements or ECMWF reanalysis. However, when averaging the
temperature derived from Koherent on a weekly basis, the agreement is within 2.5 K.
For comparison, Kerr (2002) achieved a typical standard deviation of a daily set of measurements of 0.8 K by the group scan
430 method with Brewers, in Toronto, Canada and Mauna Loa, Hawaii. Differently to Kerr (2020) the retrieval of effective
ozone temperature with Koherent is based on a parametrization with data from the two-years intercomparison in Davos,
Switzerland. It is unclear if the same parametrization can be applied for other stations worldwide, but it can at least be
applied to determine the effective ozone temperature in Davos, within 3 K on a daily basis. This has the significant
advantage that the TCO retrieval of Koherent is self-sufficient.

435

4 Conclusion and Summary

We have shown that TCO can be retrieved from direct solar ultraviolet irradiance spectra measured by an array
spectroradiometer based system (Koherent), which is a small and cost-effective instrument requiring very little maintenance.
440 The instrument was operated during two years with more than 99% data acquisition reliability. We have investigated three
different retrieval methods, such as the linear least square fit (LSF), stray light corrected LSF, Custom Double Ratio
technique (CDR) and CDR with adjusted extraterrestrial constant. The straylight corrected LSF retrieval shows a slant path
dependency, which is comparable to a double monochromator but shows a seasonal amplitude of 0.30% (Table 1). In
contrast, the seasonal amplitude of CDR is around 0.17%, but with a slant path dependency of 2.1%, which is comparable to
445 the slant path dependency of a single Brewer (Table 1).

We have shown that TCO from Koherent can either be retrieved by an absolute calibration of the Koherent spectra with the
portable world reference for ultraviolet radiation QASUME, or by an adjustment of the ETC. The calibration of the ETC
allows the instrument to be calibrated with reference instruments during intercomparison campaigns. Furthermore, absolute
TCO can be calibrated with a two-point calibration during such campaigns by additionally changing the absorption
450 coefficient to achieve the best agreement to existing network instruments (Redondas et al., 2019).

The double ratio technique using the Brewer and Dobson wavelength settings applied on Koherent spectra, further allows to
determine the effective ozone temperature within 3 K as a daily average. The retrieval of effective ozone temperature
requires a parametrization of Koherent data with an external effective ozone temperature dataset. Once the parametrization
with effective ozone temperature is provided with e.g. data of one year, the parametrization leads Koherent to serve as a
455 standalone instrument for TCO observation without the need of external supporting data such as e.g. daily effective ozone
temperature obtained from balloon soundings or other instruments.

The retrieval methods from direct ultraviolet spectra presented here are in good agreement with the performance of other
TCO instruments, e.g. Brewer or Dobson. The methods presented in this study may be applied to other array
spectroradiometer systems measuring direct solar irradiance (e.g. Pandora or BTS Solar) at other stations. Koherent serves
460 now as an instrument for operational TCO monitoring at PMOD/WRC in addition to the existing TCO instrument park
located in Davos.



Competing interests. The authors declare that they have no conflict of interest.

465 *Acknowledgement:* This research has been supported by the ESA project QA4EO, grant no. QA4EO/SER/SUB/09 and by
GAW-CH MeteoSwiss (project INFO3RS, grant no. 123001926).

Author contributions: LE and JG developed the Koherent retrieval algorithm, analysed the data and have written the
manuscript. HS and EMB were responsible for the Brewer and Dobson measurements used in this study and revised the
470 manuscript.

Data availability: The data is available from the main author (LE) on request.

Code availability: The TCO retrieval algorithm is available from the main author (LE) on request.

475 **References**

- Bass, A. M. and Paur, R. J.: The ultraviolet cross-sections of ozone, I – The measurements, II – Results and temperature dependence, in:
Atmospheric Ozone, edited by: Zerefos, C. S. and Ghazi, A., Springer, Dordrecht, The Netherlands, 606–616, https://doi.org/10.1007/978-94-009-5313-0_120, 1985.
- 480 Bodhaine, B. A., Wood, N. B., Dutton, E. G., and Slusser, J. S.: On Rayleigh Optical Depth Calculations, *J. Atmos. Ocean. Tech.*, 16,
1854–1861, 1999.
- Coddington, O. M., Richard, E. C., Harber, D., Pilewskie, P., Woods, T. N., Chance, K., et al. (2021). The TSIS-1 Hybrid Solar Reference
485 Spectrum. *Geophysical Research Letters*, 48, e2020GL091709. <https://doi.org/10.1029/2020GL091709>, 2021
- Dobson G M B 1968 Forty years research on atmospheric ozone at Oxford – a history *Appl. Optics* 387–405
- Egli, L., Gröbner, J., Hülsen, G., Bachmann, L., Blumthaler, M., Dubard, J., Khazova, M., Kift, R., Hoogendijk, K., Serrano, A., Smedley,
490 A., and Vilaplana, J. M.: Quality assessment of solar UV irradiance measured with array spectroradiometers, *Atmos. Meas. Tech.*, 9, 1553-
1567, [10.5194/amt-9-1553-2016](https://doi.org/10.5194/amt-9-1553-2016), 2016.
- Egli, L., Gröbner, J., Hülsen, G., Schill, H., and Stübi, R.: Traceable total ozone column retrievals from direct solar spectral irradiance
495 measurements in the ultraviolet, *Atmos. Meas. Tech.*, 15, 1917–1930, <https://doi.org/10.5194/amt-15-1917-2022>, March 2022.
- Evans, R. D.: Operations Handbook - Ozone Observations with a Dobson Spectrophotometer - revised version, WMO/GAW Report No.,
183, 2008.
- Gkertsi, F., Bais, F. A., Kouremeti, N., Drosoglou, T., Fountoulakis, I., and Fragkos, K.: DOAS-based total column ozone retrieval from
500 Phaethon system, *Atmospheric Environment*, 2018
- Gröbner J., Schreder J., Kazadzis S., Bais A. F., Blumthaler M., Görts P., Tax R., Koskela T., Seckmeyer G., Webb A. R., and Rembges
D.:
505 Traveling reference spectroradiometer for routine quality assurance of spectral solar ultraviolet irradiance measurements, *Appl. Opt.*, 44,
5321–5331, 2005.
- Gröbner, J. and Peter Sperfeld: Direct traceability of the portable QASUME irradiance scale to the primary irradiance standard of the PTB,
Metrologia 42 134, 2005
- 510 Gröbner, J., Kröger, I., Egli, L., Hülsen, G., Riechelmann, S., and Sperfeld, P.: A high resolution extra-terrestrial solar spectrum
determined from ground-based solar irradiance measurements, *Atmos. Meas. Tech.*, 10, 3375–3383, 2017, <https://doi.org/10.5194/amt-10-3375-2017>, 2017.
- Gröbner, J., Schill, H., Egli, L., and Stübi, R.: Consistency of total column ozone measurements between the Brewer and Dobson
515 spectroradiometers of the LKO Arosa and PMOD/WRC Davos, *Atmos. Meas. Tech.* 3319–3331,
<https://doi.org/10.5194/amt-14-3319-2021>, 2021
- Huber, M., Blumthaler, M., Ambach, W., and Staehelin, J.: Total atmospheric ozone determined from spectral measurements of direct
520 solar UV irradiance, *J. Geophys. Res.*, 94, 53–56, [10.1029/94gl02836](https://doi.org/10.1029/94gl02836), 1995.



- Herman, J., Evans, R., Cede, A., Abuhassan, N., Petropavlovskikh, I., McConville, G., Miyagawa, K., and Noiro, B.: Ozone comparison between Pandora #34, Dobson #061, OMI, and OMPS in Boulder, Colorado, for the period December 2013–December 2016, *Atmos. Meas. Tech.*, 10, 3539–3545, <https://doi.org/10.5194/amt-10-3539-2017>, 2017.
- 525 Hülsen, G., Gröbner, J., Nevas, S., Sperfeld, P., Egli, L., Porrovecchio, G., and Smid, M.: Traceability of solar UV measurements using the QASUME reference spectroradiometer, *Appl. Optics*, 55, 7265–7275, 2016
- Kerr, J. B., Asbridge, I. A., Evans, W. F. J.: Intercomparison of total ozone measured by the Brewer and Dobson Spectrophotometers at Toronto *J. Geophys. Res.*, 93(D9), 11,129–11,140, 1988
- 530 Kerr, J. B., McElroy, C. T., Olafson, R. A.: Measurements of total ozone with the Brewer spectrophotometer *Proc. Quad. Ozone Symp.*, 1980, J. London (ed.), Natl. Cent. for Atmos. Res., Boulder CO, 74-79, 1981
- 535 Kerr, J. B., McElroy, C. T., Wardle, D. I., Olafson, R. A., Evans, W. F. J.: The automated Brewer Spectrophotometer *Proceed. Quad. Ozone Symp.* in Halkidiki, C.S. Zerefos and A. Ghazi (Eds.), D. Reidel, Norwell, Mass., pp. 396-401, 1985
- Kerr, J. B.: New methodology for deriving total ozone and other atmospheric variables from Brewer spectrophotometer direct sun spectra, *J. Geophys. Res.*, 107(D23), 4731, <https://doi.org/10.1029/2001JD001227>, 2002.
- 540 Komhyr, W. D., Grass, R. D., and Leonard, R. K.: Dobson Spectrophotometer 83: A Standard for Total Ozone Measurements, 1962–1987, *J. Geophys. Res.*, D7(94), 9847–9861, 1989.
- 545 Köhler, U., Nevas, S., McConville, G., Evans, R., Smid, M., Stanek, M., Redondas, A., and Schöenborn, F.: Optical characterisation of three reference Dobsons in the ATMOZ Project – verification of G. M. B. Dobson’s original specifications, *Atmos. Meas. Tech.*, 11, 1989-1999, <https://doi.org/10.5194/amt-11-1989-2018>.
- 550 Kouremeti N., A. Bais, S. Kazadzis, M. Blumthaler, and R. Schmitt, Charge-coupled device spectrograph for direct solar irradiance and sky radiance measurements, *Appl. Opt.*, 47, 10, 1594-1607, 2008.
- Molina, M. J., and F. S. Rowland: Stratospheric sink for chlorofluoromethanes-Chlorine atom catalyzed destruction of ozone, *Nature*, 249, 810–812, 1974.
- 555 Redondas A, Evans R, Stübi R, Köhler U and Weber M 2014 Evaluation of the use of five laboratory-determined ozone absorption cross sections in Brewer and Dobson retrieval algorithms *Atmos. Chem. Phys.*, 14, 1635–1648
- Redondas, A., León-Luís, S. F., López-Solano, J., Berjón, A., and Carreño, V.: Thirteenth Intercomparison Campaign of the Regional Brewer Calibration Center Europe, Joint publication of State Meteorological Agency (AEMET), Madrid, Spain and World Meteorological Organization (WMO), Geneva, Switzerland, WMO/GAWReport No. 246, <https://doi.org/10.31978/666-20-018-3>, 2019.
- 560 Staehelin, J., Viatte, P., Stübi, R., Tummon, F., and Peter, T.: Stratospheric ozone measurements at Arosa (Switzerland): history and scientific relevance, *Atmos. Chem. Phys.*, 18, 6567–6584, <https://doi.org/10.5194/acp-18-6567-2018>, 2018.
- 565 Stübi, R., Schill, H., Klausen, J., Vuilleumier, L., and Ruffieux, D. C.: Reproducibility of total ozone column monitoring by the Arosa Brewer spectrophotometer triad, *J. Geophys. Res.-Atmos.*, 122, 4735–4745, <https://doi.org/10.1002/2016JD025735>, 2017a.
- Stübi, R., Schill, H., Klausen, J., Vuilleumier, L., Gröbner, J., Egli, L., and Ruffieux, D.: On the compatibility of Brewer total column ozone measurements in two adjacent valleys (Arosa and Davos) in the Swiss Alps, *Atmos. Meas. Tech.*, 10, 4479–4490, <https://doi.org/10.5194/amt-10-4479-2017>, 2017b.
- 570 Stübi, R., Schill, H., Klausen, J., Maillard Barras, E., and Haefele, A.: A fully Automated Dobson Sun Spectrophotometer for total column ozone and Umkehr measurements, *Atmos. Meas. Tech.*, <https://doi.org/10.5194/amt-14-5757-2021>.
- 575 Serdyuchenko, A., Gorshelev, V., Weber, M., Chehade, W., and Burrows, J. P.: High spectral resolution ozone absorption crosssections– Part 2: Temperature dependence, *Atmos. Meas. Tech.*, 7, 625–636, <https://doi.org/10.5194/amt-7-625-2014>, 2014.
- Solomon, S.: Stratospheric ozone depletion: A review of concepts and history, *Rev. Geophys.*, 37, 275–316, 1999
- 580 Thompson, D., Seidel, D., Randel, W. et al. The mystery of recent stratospheric temperature trends. *Nature* 491, 692–697 (2012). <https://doi.org/10.1038/nature11579>
- WMO (World Meteorological Organization), *Scientific Assessment of Ozone Depletion: 2018*, Global Ozone Research and Monitoring Project – Report No. 58, 588 pp., Geneva, Switzerland, 2018.
- 585 Zuber, R., Ribnitzky, M., Tobar, M., Lange, K., Kutscher, D., Schrempf, M., Niedzwiedz, A., and Seckmeyer, G.: Global spectral irradiance array spectroradiometer validation according to WMO, *Measurement Science and Technology*, 2018a.
- Zuber, R., Sperfeld, P., Riechelmann, S., Nevas, S., Sildoja, M., and Seckmeyer, G.: Adaption of an array spectroradiometer for total ozone column retrieval using direct solar irradiance measurements in the UV spectral range, *Atmos. Meas. Tech.*, 11, 2477–2484, <https://doi.org/10.5194/amt-11-2477-2018>, 2018, 1-12, [10.5194/amt-2017-240](https://doi.org/10.5194/amt-2017-240), 2018b
- 590



Zuber, R., Köhler, U., Egli, L., Ribnitzky, M., Steinbrecht, W., and Gröbner, J.: Total ozone column intercomparison of Brewers, Dobsons, and BTS-Solar at Hohenpeißenberg and Davos in 2019/2020, *Atmos. Meas. Tech.*, 14, 4915–4928, <https://doi.org/10.5194/amt-14-4915-2021>, 2021.

595

Comparison with Brewer 156

Instrument	Longterm Offset [%]	Seasonal Amplitude [%]	Slant Path (Min-Max) [%]
Koherent: LSF 305 nm - 345 nm	0.26	1.17	4.42
Koherent: LSF 310 nm - 345 nm	0.02	0.86	2.18
Koherent: LSF Stray Light Corrected	0.67	0.30	0.46
Koherent: CDR	0.02	0.17	2.13
Koherent: CDR ETC Adjusted	-0.59	0.34	2.12
Koherent: LSF/CDR Combined	0.05	0.08	1.62
Brewer 040	-0.29	0.16	1.52
Brewer 072	-0.15	0.25	2.53
Brewer 163	0.21	0.02	0.35
Dobson 101	0.06	0.17	1.42
QASUME	1.13	0.22	0.18

Table 1: Comparison of the performance of different TCO retrievals for Koherent and other TCO instruments. The double monochromator Brewer 156 is chosen as the reference instrument for the comparison. LSF stands for Least Square Fit retrieval and CDR for Custom Double Ratio technique. The offsets indicate the long-term bias over the entire period of comparison (1 oct 2019 to 30 Sep 2021). The seasonal amplitude indicates the amplitude of a sinusoidal fit of the TCO relative differences over the years (see Figure 5) and the slant path quantification indicates the difference of the ozone slant path dependency of a quadratic fit of the TCO relative differences (see Figures 3 and 4).

605



Picture 1: The lens-based telescope of Koherent on a sun tracker at the measurement platform of PMOD/WRC. The telescope is connected by an optical fiber to the BTS array spectroradiometer in the temperature stabilized box.

610

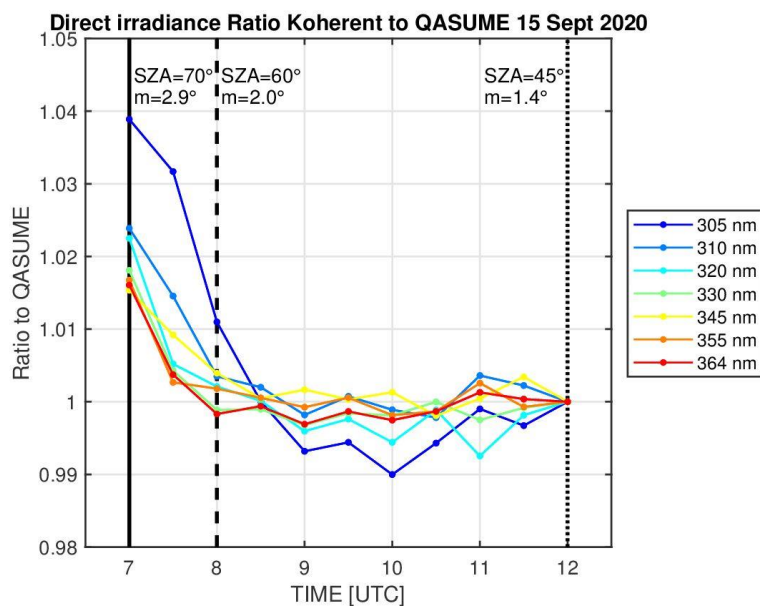


Figure 1: Comparison between QASUME and Coherent spectra on morning of 15 September 2020 displaying the direct irradiance ratios for individual wavelength bands within ± 2.5 nm. The ratios are normalized to the ratio at 12 UTC (noon). The solar zenith angles (SZA) and the air mass (m) for UTC 7, 9, 12 (noon) are indicated by vertical lines.

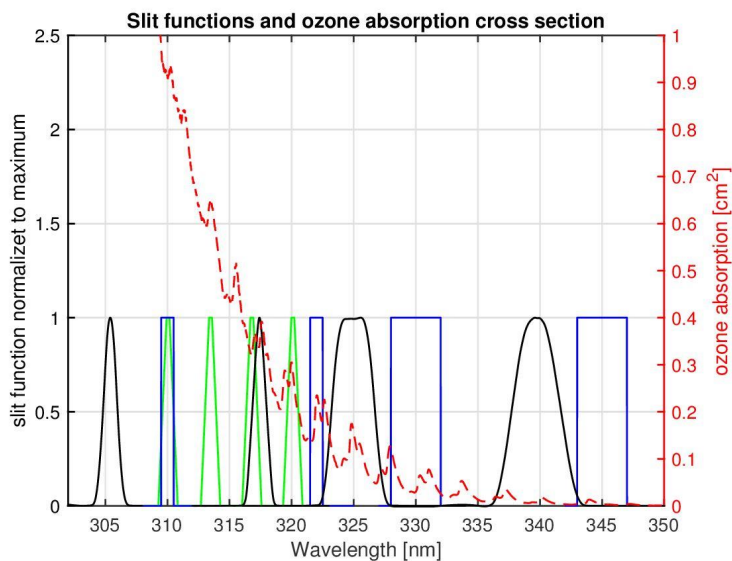
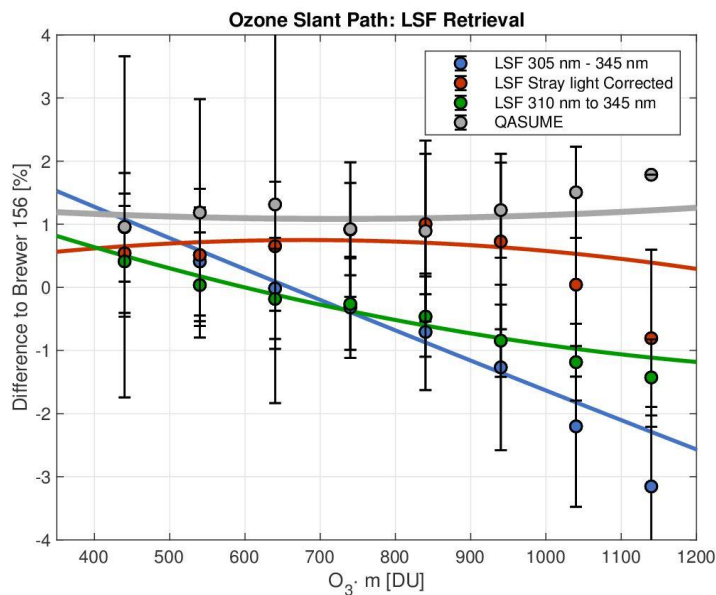
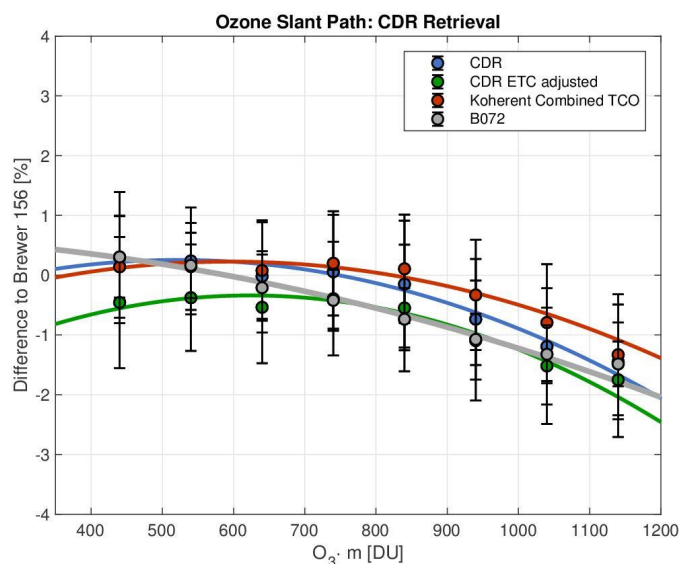


Figure 2: Slit functions of the Custom Double Ratio technique for Coherent (blue), the trapezoidal slit functions of the Brewer (green) and the measured slit function of Dobson 101 (black). The red dashes line indicates the ozone absorption cross section SG14 at effective temperature of 228 K.

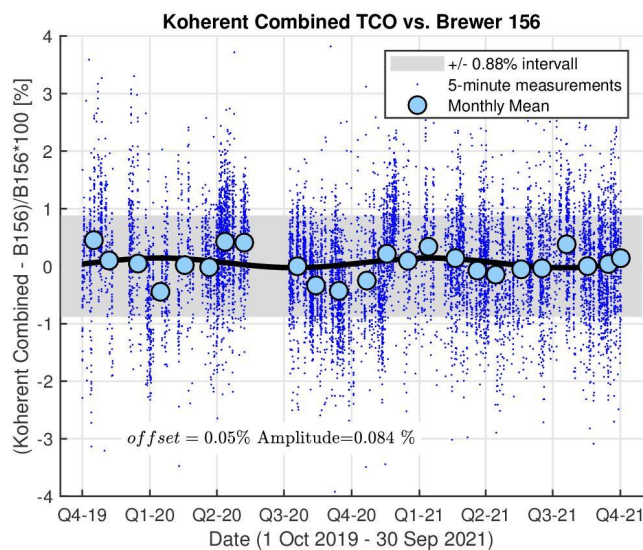


625 *Figure 3: Ozone slant path comparison of Koherent LSF retrieval with the double monochromator Brewer 156 for the wavelength range of 305 – 345 nm retrieval (blue), the wavelength range of 310 – 345 nm retrieval (green), and stray light corrected retrieval (red). For comparison, the performance of QASUME is indicated in grey. The lines indicate quadratic fits to all measurements, which are not specifically shown. The circles are averages on 100 DU bins.*

630



635 *Figure 4: Ozone slant path comparison of Koherent CDR retrieval with the double monochromator Brewer 156 for standard CDR retrieval (blue), ETC adjusted CDR retrieval (green), and LSF/CDR combined retrieval (red). For comparison, the performance of the single monochromator Brewer 072 is indicated in grey. The lines indicate quadratic fits to all measurements, which are not specifically shown. The circles are averages on 100 DU bins.*



640

Figure 5: Relative difference between Koherent (LSF and CDR combined) and Brewer 156 double monochromator. The small blue points indicate the synchronized measurements in five minute interval. The light blue circles are monthly means. The grey area indicates the standard deviation of the relative difference between the three retrievals used for the combined product. The seasonal amplitude is 0.084% with a long term offset of 0.05%.

645

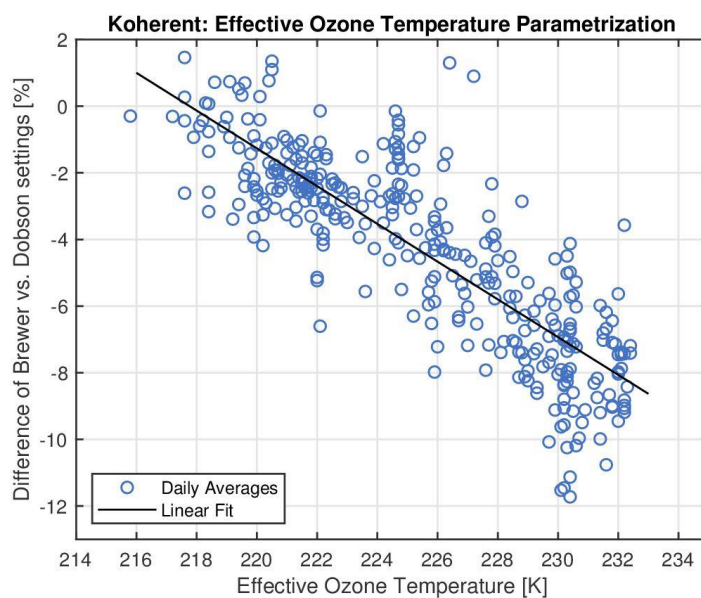


Figure 6: Parametrization of the relative differences between CDR retrieval using Dobson and Brewer wavelength and slit function settings at 228 K effective ozone temperature, with daily effective ozone temperature from balloon soundings. The linear fit exhibits a slope of 0.5%/K indicating the sensitivity of the differences to effective ozone temperature.

650



655

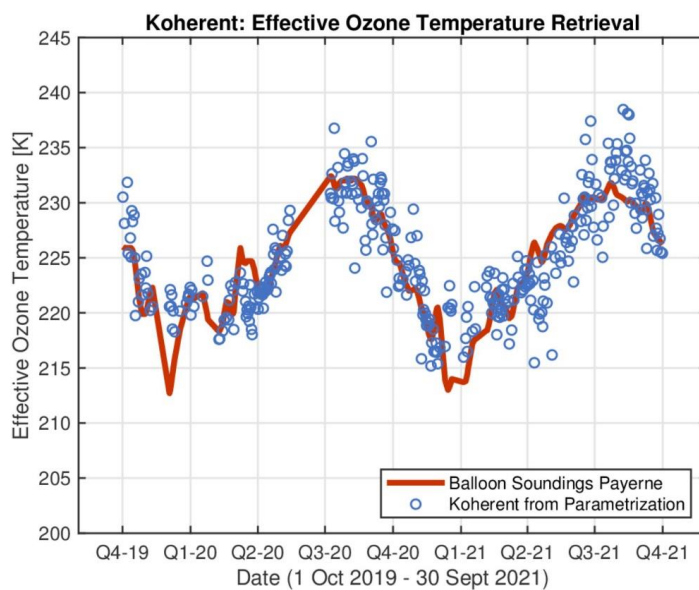


Figure 7: Effective ozone temperature derived from the parametrization of differences between CDR retrieval from Brewer and Dobson wavelength and slit function settings.

660